UNIVERSITY OF THESSALY
SCHOOL OF ENGINEERING
DEPARTMENT OF MECHANICAL ENGINEERING

Diploma Thesis

Experimental Study of the Effect of Pre-existing Plastic Deformation on Fatigue Crack Growth Rate in S355MC Steel

by

ARTEMIOS TZAFAS

Submitted in partial fulfillment of the requirements for the degree of Diploma in Mechanical Engineering at University of Thessaly

Volos, 2021

Approved by the Committee on Final Examination:

Advisor	Dr. Alexis Kermanidis, Associate Professor, Department of Mechanical Engineering, University of Thessaly
Member	Dr. Spyros Karamanos, Professor, Department of Mechanical Engineering, University of Thessaly
Member	Dr. Gregory Haidemenopoulos, Professor, Department of Mechanical Engineering, University of Thessaly

Acknowledgements

First of all, I would like to express my sincere gratitude to the supervisor of this thesis, Associate Professor Alexis Kermanidis for trusting me with this subject and involving me with a university research project. I would also like to thank Professor Kermanidis' PhD student, Christos Prosgolitis, for his invaluable scientific support throughout my work. Finally, I thank my family and friends for standing by my side in all my endeavors.

Abstract

A wide variety of components that are used across all manufacturing areas are constructed through cold-formed steel. The term cold-formed is commonly referred to steel products shaped by cold-working processes carried out near room temperature such as rolling, pressing, stamping, bending, etc. Cold-forming changes the mechanical properties of the material especially around bent sections. As the material is being plastically deformed, phenomena such as work hardening take place and residual stresses are induced.

Fatigue damage is a very common type of mechanical failure that is accumulated in materials by the cyclic application of loads. Mechanical components that are susceptible to fatigue undergo frequent inspections according to estimated fatigue life predictions. However, cold-formed components make such predictions challenging as their behavior alters along their plastically deformed areas.

In order to characterize how material behavior changes due to plastic deformation, a European project called FASTCOLD aims to develop fatigue design rules for cold-formed steel members focusing on racking systems. The objective of this thesis, being a part of the aforementioned project, is to simulate cold-formed material through pre-existing plastic deformation and study how fatigue crack growth is affected in S355MC steel.

After investigating the phenomenon and building theoretical basis, test specimens are designed and test parameters are calculated according to standards in order to perform reliable testing. Then, fatigue crack growth tests are performed using laboratory equipment and after data acquisition and processing, the results are discussed and evaluated. These results are then carefully examined to interpret crack growth behavior under different pre-strain levels and a couple loading conditions. In addition, some (although incomplete) testing was undergone to study the crack closure effect performing crack opening force measurements within a range of crack lengths across the tested pre-strain levels.

Such research is of great importance in order to understand the mechanical response of plastically pre-strained material and ensure the design of safe mechanical structures while providing valuable insight into how and why components fail.

Περίληψη

Μια μεγάλη ποικιλία εξαρτημάτων που χρησιμοποιούνται σε όλους τους κατασκευαστικούς τομείς παράγονται μέσω της ψυχρής έλασης. Ο όρος ψυχρή έλαση αναφέρεται συνήθως σε προϊόντα χάλυβα που διαμορφώνονται μέσω διεργασιών που πραγματοποιούνται κοντά σε θερμοκρασίες δωματίου. Η ψυχρή έλαση αλλάζει τις μηχανικές ιδιότητες του υλικού ειδικά γύρω απο περιοχές που υπέστησαν πλαστική παραμόρφωση.

Η κόπωση είναι πολύ κοινός τύπος μηχανικής αστοχίας που συσσωρεύεται στα υλικά με την κυκλική εφαρμογή φορτίων. Τα μηχανικά εξαρτήματα που είναι ευπαθή σε κόπωση υποβάλλονται σε συχνές επιθεωρήσεις βασιζόμενες σε εκτιμήσεις για την διάρκεια ζωής σε κόπωση. Ωστόσο, τα ψυχρά διαμορφωμένα εξαρτήματα δυσκολεύουν την πραγματοποίηση τέτοιων προβλέψεων καθώς η μηχανική συμπεριφορά τους αλλάζει γύρω απο τις πλαστικά παραμορφωμένες περιοχές τους.

Προκειμένου να χαρακτηριστεί ο τρόπος με τον οποίο αλλάζει η συμπεριφορά του υλικού λόγω πλαστικών παραμορφώσεων, ένα ευρωπαϊκό ερευνητικό έργο εν ονόματι FASTCOLD στοχεύει στην ανάπτυξη κανόνων σχεδιασμού με γνώμονα την κόπωση για την κατασκευή μεταλλικών εξαρτημάτων μέσω της ψυχρής έλασης εστιάζοντας στα συστήματα ραφιών. Ο σκοπός αυτής της διατριβής, που αποτελεί μέρος του προαναφερθέντος έργου, είναι να προσομοιώσει το ψυχρά διαμορφωμένο υλικό μέσω της προϋπάρχουσας πλαστικής παραμόρφωσης και να μελετήσει πως επηρεάζεται η ανάπτυξη ρωγμών κόπωσης σε χάλυβα S355MC.

Μετά τη διερεύνηση του φαινομένου και την ανάπτυξη θεωρητικής βάσης, σχεδιάζονται τα δοκίμια που θα χρησιμοποιηθούν για τα πειράματα και υπολογίζονται οι πειραματικοί παράμετροι σύμφωνα με τα αντίστοιχα πρότυπα για την διεξαγωγή αξιόπιστων δοκιμών. Στη συνέχεια, πραγματοποιούνται δοκιμές ανάπτυξης ρωγμών κόπωσης χρησιμοποιώντας εργαστηριακό εξοπλισμό και ύστερα από την συλλογή και επεξεργασία των δεδομένων, εξετάζονται και αξιολογούνται τα αποτελέσματα. Έπειτα, τα αποτελέσματα αυτά αναλύονται προσεκτικά για να ερμηνεύσουμε τη συμπεριφορά της ανάπτυξης ρωγμών υπό διαφορετικά επίπεδα πλαστικής παραμόρφωσης και δύο συνθήκες φόρτισης. Επιπλέον, πραγματοποιήθηκαν ορισμένες (αν και ελλιπείς) εργαστηριακές δοκιμές μελετώντας το φαινόμενο κλεισίματος της ρωγμής υποβάλλοντας τα δοκίμια σε μετρήσεις της δύναμης ανοίγματος ρωγμής εντός ενός εύρους μηκών στα εξεταζόμενα επίπεδα πλαστικής παραμόρφωσης.

Τέτοιου είδους έρευνες έχουν ιδιαίτερη σημασία για την κατανόηση της μηχανικής απόκρισης του πλαστικώς προεντεταμένου υλικού και τη διασφάλιση του σχεδιασμού ασφαλών μηχανικών κατασκευών, παρέχοντας παράλληλα πολύτιμες πληροφορίες για την κατανόηση του τρόπου και των αιτιών που προκαλούν μηχανικές αστοχίες.

Contents

Chapter 1: Introduction 9
1.1 Background and Motivation 9
1.2 Thesis Outline 9
Chapter 2: Specimen Design and Testing Framework 10
2.1 Material 10
2.2 Plate Fabrication and Specimen Design 10
2.3 Test Parameters 13
Chapter 3: Experimental Procedure and Data Processing 17
3.1 Specimen Preparation 17
3.2 Experimental Setup 18
3.3 Data Processing 20
3.4 Opening force measurements 20
Chapter 4: Experimental Results 23
4.1 Fatigue Crack Growth Results 23
4.2 Opening Force Results 26
4.3 Discussion 27
Chapter 5: Conclusions and Future Directions 29
References 31

Figures

Figure 2.1 Plate geometry of the pre-stretched panel 10
Figure 2.2 Characteristic longitudinal and transverse strain map 11
Figure 2.3 Standard Compact Tension Specimen 11
Figure 2.4 Specimen dimensions (mm) 12
Figure 2.5 Example of specimen placement on strain maps 12
Figure 2.6 Specimen sample 13
Figure 2.7 Paris law for crack growth da/dN as function of the stress intensity factor range ΔK 14
Figure 3.1 Prepared specimen 17
Figure 3.2 Specimen ready for testing 18
Figure 3.3 Specimen ready for testing (overlay) 18
Figure 3.4 Instron Fatigue Testing System 19
Figure 3.5 COD gauge clipped on a specimen fitted on the fatigue testing machine 19
Figure 3.6 DSLR camera and macro lens 19
Figure 3.7 Crack examination 21
Figure 3.8 Crack initiation snapshot 21
Figure 4.1a da/dN diagram of reference and pre-strained material for stress ratio $R = 0.1$. 23
Figure 4.2a da/dN diagram of reference and pre-strained material for stress ratio $R = 0.5$. 23
Figure 4.1b Paris curves of reference and pre-strained material for stress ratio $R = 0.1$ 24
Figure 4.2b Paris curves of reference and pre-strained material for stress ratio $R = 0.5$ 24
Figure 4.3 Stress ratio R effect on crack growth rates for reference material 25
Figure 4.4 Stress ratio R effect on crack growth rates for 8-9% pre-strain level 25
Figure 4.5 Stress ratio R effect on crack growth rates for 12-13% pre-strain level 26
Figure 4.6 Stress ratio R effect on crack growth rates for 15-16% pre-strain level 26
Figure 4.7 Pre-strain effect on crack opening force Po 27
Figure 4.8 a-N curve for 12-13% pre-strain level 28

Tables

Table 2.1 Chemical composition (%) of S355MC steel 10

Table 2.2 List of testing parameters..... 15

Table 3.1 Raw $d\alpha/dN$ data sample from I3 specimen (12-13% pre-strain level, stress ratio $R = 0.1$) 20

Table 3.2 Raw Po measurement data sample for J2 specimen (8-9% pre-strain level, stress ratio $R = 0.1$) 22

Chapter 1: Introduction

1.1 Background and Motivation

Material fatigue is a phenomenon where structures fail when subjected to a cyclic load. This type of structural damage occurs even when the experienced stress range is far below the static material strength. Fatigue is the most common source behind failures of mechanical structures [1]. Therefore, it is important to have methods to predict the fatigue life of a material in order to schedule inspections and repairs to prevent catastrophic failure.

Fatigue has traditionally been associated with the failure of metal components. A great part of these components are manufactured through cold-forming. Cold-formed steel is commonly used in the construction industry and generally all areas of manufacturing as it easy to mass produce and provides high strength and stiffness compared to its weight. When a steel section is cold-formed from flat sheet or strip, the yield strength, and to a lesser extent the ultimate strength, are increased as a result of cold working, particularly in the bends of the section [2]. That changes the mechanical properties of the material resulting in a loss of ductility making it more brittle [8]. Also, bent areas in cold-formed parts induce residual stresses and the change in geometry creates stress concentration fields accelerating fatigue crack growth. Therefore, it is important to characterize how materials respond to plastic deformation aiming to predict their behavior under the effect of fatigue.

This thesis is has been performed in the frame of a 42-month long research project called FAtigue STrength of COLD-formed structural steel (FASTCOLD) and it aims to develop fatigue design rules for cold-formed steel members and their connections. It specifically focuses to applications for the logistic industry (i.e. racking systems) which are urgently needed for the safe design of rack structures for present and future demands [3]. Specifically, the objective of this thesis is to study the effect of pre-existing plastic deformation on fatigue crack growth rate in S355MC steel.

1.2 Thesis Outline

The remainder of this thesis is organized as follows.

In CHAPTER 2, we briefly describe how test specimens are designed from sheet material and how the theoretical basis and the parameters for testing are deduced.

CHAPTER 3 is devoted to the methodology of fatigue crack growth testing and data acquisition.

In CHAPTER 4 and 5 we present and evaluate the results and discuss our assumptions.

Finally, CHAPTER 6 summarizes our conclusions and suggests some directions for future research.

Chapter 2: Specimen Design and Testing Framework

2.1 Material

The material that was used for the fatigue crack growth testing is S355MC steel which is a very commonly used structural grade of steel. ‘S’ states the fact that it is structural steel, ‘355’ relates to the minimum yield strength (tested at a thickness of 16 mm) [4], ‘M’ means that it has been subjected to thermo mechanical rolling and ‘C’ means that the steel has been cold drawn [5]. Table 2.1 depicts the chemical composition of S355MC steel.

Table 2.1 Chemical composition (%) of S355MC steel

C	Si	Mn	P	S	V	Nb	Ti	Al
max 0.12	max 0.5	max 1.5	max 0.025	max 0.02	max 0.2	max 0.09	max 0.15	min 0.015

This grade of steel offers good welding properties and strength while being suitable for cold forming [6]. The supports that are related to FASTCOLD project are manufactured through cold rolling so using S355MC steel is appropriate for the application.

2.2 Plate Fabrication and Specimen Design

As it was previously hinted, the raw material comes in rolled sheet form. Plates are cut which are then deformed to the desired amounts. The geometry of each plate (see Figure 2.1) produces areas of different strain percentages. In order to visualize these areas, strain maps are produced optically which depict the amount of deformation using strain percentages in longitudinal and transverse direction (see Figure 2.2).

These pre-stretched plates and their accompanying strain maps where designed and supplied by the laboratory of RWTH Aachen University which is another partner of the FASTCOLD project from Germany.

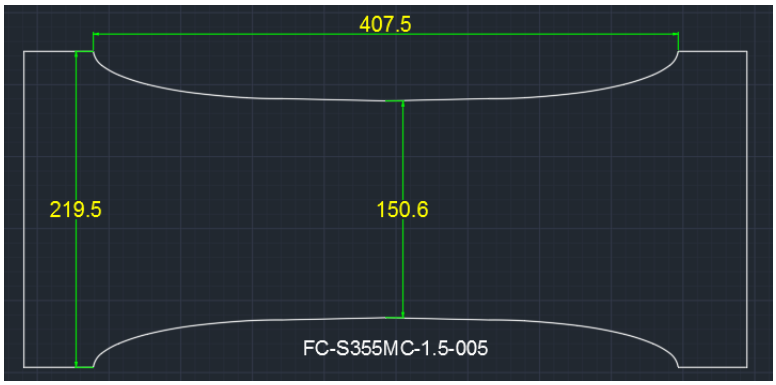

Figure 2.1 Plate geometry of the pre-stretched panel

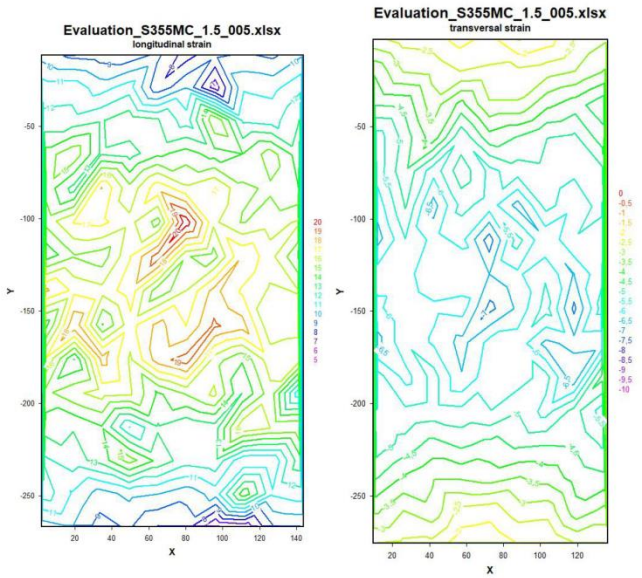

Figure 2.2 Characteristic longitudinal and transverse strain map

The next step is specimen design. The type of specimen that was used for testing is the compact tension specimen (C(T)). The C(T) specimen has the advantage over other specimen types in that it requires the least amount of material to evaluate crack growth behavior [7]. So, smaller specimens are favorable for maximizing material utilization. E 647 standard provides the specimen dimensions as shown in Figure 2.3.

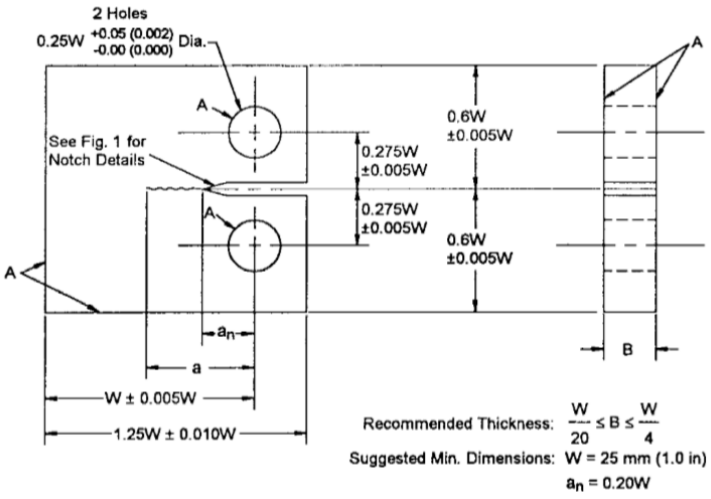

Figure 2.3 Standard Compact Tension Specimen

Therefore, given that the plates are 1.5 mm thick and we want to fit as many specimens as possible on each one of them, the final specimen dimensions are reached as shown in Figure 2.4. The geometry on the right side of the notch allows the crack opening displacement (COD) gauge to be clipped securely.

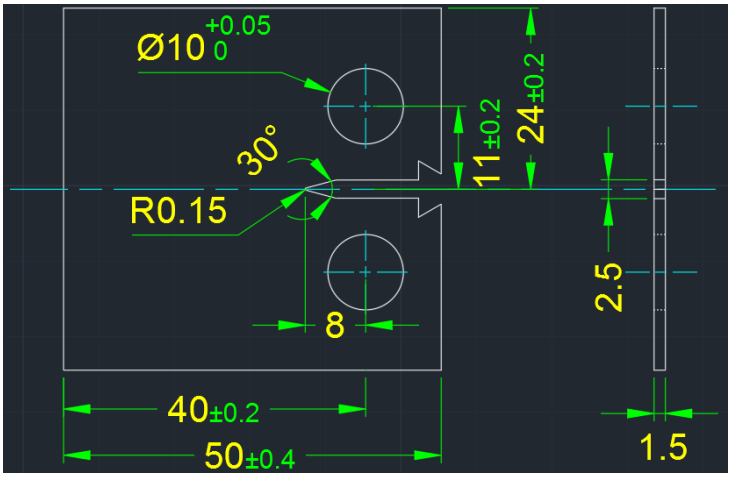

Figure 2.4 Specimen dimensions (mm)

In order to study the effect of plastic deformation on crack growth rates, specimens with different strain amounts are needed. Given that each plate has a certain range of strain percentages in each direction, groups of specimens are formed with at least 2% difference in longitudinal strain in order to produce observable difference in crack growth rates. With that in mind, specimens are placed on each map as shown in Figure 2.5.

E1P: 8-9 (L%), 2-3 (T%)
B6P: 12-13 (L%), 4-5 (T%)
B7P: 13 (L%), 4-5.5 (T%)
C8P: 15-16 (L%), 5-6 (T%)
C9P: 15-16 (L%), 6-6.5 (T%)
D3T: 5.5-6 (L%), 17-19 (T%)
D4T: 5.5-6 (L%), 16-18 (T%)
B8P: 12-13 (L%), 4.5-5 (T%)
B9P: 12-13 (L%), 4-5 (T%)
E2P: 8-9 (L%), 2-2.5 (T%)

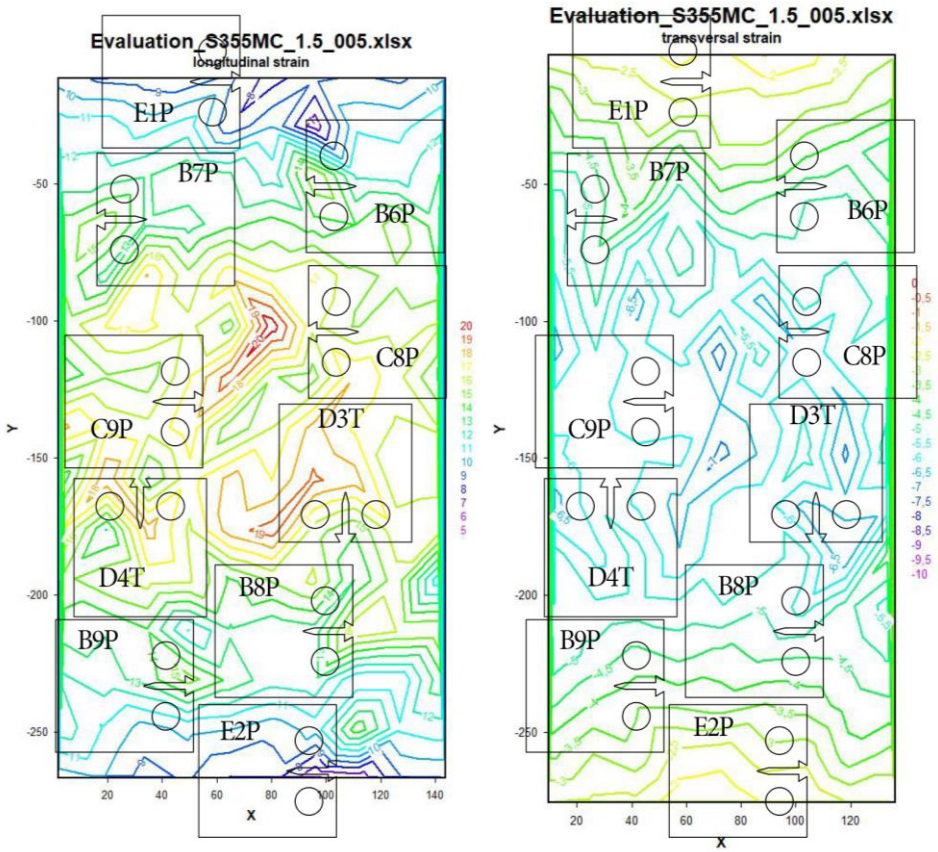

Figure 2.5 Example of specimen placement on strain maps

It is important to mention that each specimen is placed in such way that the crack path resides in an area of uniform (longitudinally) deformation. The specimens that were used for this study have parallel stretching and loading directions. In other words, the direction in

which the plates where plastically deformed is parallel to the direction of the cyclic loads that were applied during testing each specimen.

The plates (with each corresponding map) are then sent to be cut. Each specimen is machined using electric discharge as it is the most accurate method with the ability to produce extremely small notch root radiuses (ρ<0.25 mm) while leaving little to none residual stresses behind as they can affect the crack propagation especially around the notch area.

Each specimen is carefully measured upon arrival to ensure that tolerances are met, providing accurate input for calculating the test parameters. A specimen sample can be seen in Figure 2.6.

Figure 2.6 Specimen sample

2.3 Test Parameters

After all that preparation, test parameters must be determined. There are two types of tests that were performed, one to determine crack growth rates (da/dN) and one to measure the crack opening force (P_o) at various crack lengths.

First of all, some criteria have to be set to ensure that testing will be performed according to the ASTM E647 standard [7] so that test results are valid. For that, the following equations are needed:

$$\Delta K = (1 - R)K_{max} \text{ for } R \geq 0 \tag{2.1}$$

$$(W - a) \geq (4/\pi)(K_{max}/\sigma_{YS})^2 \tag{2.2}$$

$$\Delta K = \frac{\Delta P}{B\sqrt{W}} \frac{(2 + \boldsymbol{a})}{(1 - \boldsymbol{a})^{3/2}} (0.886 + 4.64\boldsymbol{a} - 13.32\boldsymbol{a}^2 + 14.72\boldsymbol{a}^3 - 5.6\boldsymbol{a}^4) \tag{2.3}$$

where $\boldsymbol{\alpha} = a/W$

Now, ΔK is the stress intensity factor range ($\Delta K = K_{max} - K_{min}$), R is the force ratio, also called stress ratio ($R = P_{min}/P_{max}$) and W, B and a are specimen dimensions as depicted in Figure 2.3.

For our tests, we need to calculate the minimum stress intensity factor range to enable a crack to propagate (ΔK_{th}) within our specimen and the maximum stress intensity factor ($K_{\max}$) for which the Linear Elastic Fracture Mechanics (LEFM) criteria are met.
For a given material and a set of test conditions, crack growth behavior can be described by the relationship between cyclic crack growth rate da/dN and stress intensity range ΔK. At intermediate values ofΔK, there is a straight line (on a log-log plot) represented by the following equation:

$$\frac{da}{dN} = C(\Delta K)^m \tag{2.4}$$

where C is a constant and m is the slope on the log-log plot as depicted in Figure 2.7. That equation, and the following curve, is named after Paul Paris who first used it in the early 1960s [8].

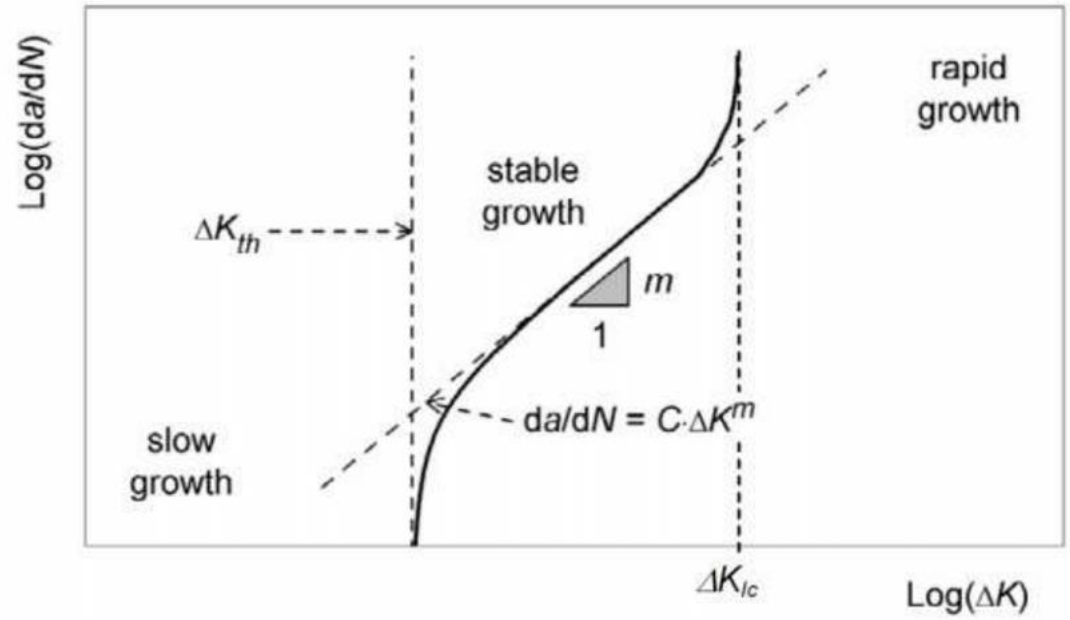

Figure 2.7 Paris law for crack growth da/dN as function of the stress intensity factor range ΔK

It is known that in a very similar material (S355 J2), Paris law applies at a value of $\Delta K_{th} \cong 10\ MPa\sqrt{m}$ and above [9]. So, for this analysis, we can assume that crack growth rates fall into the straight line part of the Paris curve at a value of $\Delta K \cong 12\ MPa\sqrt{m}$. Also, rapid growth at high ΔK involves macroscopic plastic yielding where LEFM criteria are inapplicable as the plastic zone becomes so large that it eliminates the K-field and the theoretical limitations of the K concept are exceeded [8]. Therefore, K_{max} can be calculated as an upper limit using Eq. 2.2 and specimen dimensions (see Figures 2.3 and 2.4). In this case, LEFM criteria are met for $K_{max} \leq 48\ MPa\sqrt{m}$.

In addition, using Eqs. 2.1, 2.2 and 2.3 and solving for a leads to an inequality which can be used to calculate a_{final} (final crack length under LEFM) as a useful reference point in data plotting later on in the process.

At this point it should be mentioned that another study had taken place prior to this one performing tests on the same material with no deformation whatsoever as reference [10]. Thus, for comparison reasons, some test parameters, such as loading conditions, have already been set by those previous tests. To be more specific, tests were performed for stress ratios of $R = 0.1$ and $R = 0.5$. Moreover, in order to be able to compare the data between reference and deformed material we must ensure that the crack propagates under the same applied stress. Thus, the following relation is true:

$$\begin{aligned} \sigma_r &= \sigma_d, \\ P_r/B_r &= P_d/B_d, \\ P_d &= (B_d/B_r)P_r \end{aligned} \tag{2.5}$$

where the indicators r and d refer to reference and deformed material respectively. The forces (P_{min}, P_{max}) that were used for fatigue testing on the reference material are known, so the forces for testing on the deformed material can be calculated using Eq. 2.5 as the specimen thickness (B) changes with different amounts of plastic deformation.

Having all of that ready, the forces for each test specimen are calculated which is ultimately what is used for input to the fatigue testing machine. A list of the specimens and testing parameters used in this study can be seen in Table 2.2.

Table 2.2 List of testing parameters

A/A	Specimen	LONG Strain (%)	TRANS Strain (%)	Thickness (mm)	Stress Ratio (R)	Number of Specimens
1	J1	8-9	-2.5-3	1.435	0.1	
2	J2	8-9	-2.5-3	1.423	0.1	
3	J3	8-9	-2.5-3	1.43	0.1	**6**
4	J4	8-9	-2.5-3	1.435	0.5	
5	L1	8-9	-2.5-3	1.464	0.5	
6	L2	8-9	-2-2.5	1.462	0.5	
7	I1	12-13	-4.5	1.415	0.1	
8	I2	12-13	-4-4.5	1.413	0.1	
9	I3	12-13	-3.5-4	1.421	0.1	**6**
10	K1	12-13	-3.5-4.5	1.43	0.5	
11	K2	12-13	-3.5-4	1.437	0.5	
12	L3	12-13	-4-5	1.434	0.5	
13	I6	15-16	-5.5	1.41	0.1	
14	J5	15-16	-5	1.41	0.1	
15	J6	15-16	-5-5.5	1.403	0.1	**6**
16	J7	15-16	-5.5	1.391	0.5	
17	J8	15-16	-5-5.5	1.391	0.5	
18	K3	15-16	-6	1.416	0.5	

Opening force (P_o) measurements were performed only for stress ratio $R = 0.1$ as crack closure effect becomes less evident with the increase of R and loading forces. It is also important to mention that (as seen in Table 2.2) each set of test parameters must be tested at least three times to ensure that test results, and therefore the conclusions derived from them, are accurate.

After all of that, the specimens are ready for actual fatigue testing.

Chapter 3: Experimental Procedure and Data Processing

3.1 Specimen Preparation

Having the specimens ready and their dimensions measured, the first step before testing is marking them. Crack length is frequently checked through a DSLR camera during the test and an appropriate lens is used to provide adequate magnification. Thus, in order to determine the actual length, some kind of scale must be used.

The scale that was used comes in the form of stickers with dots of fixed diameter. These dots are then placed near the notch of each specimen around the precrack area. The precrack itself is a natural crack that is formed on the beginning of each test under the same testing forces in order to reach crack growth rates that fall into the straight line part of the Paris curve. It is important to place the aforementioned stickers as close as possible to the expected crack path without obstructing its visibility. If needed, the notch area can be cleaned with acetone to provide better adherence to the sticker and improved visibility to the camera. In case of rust, a very fine sandpaper can be used to clean the notch surface area. Additionally, it is useful to mark a small line roughly around the precrack length as a point of reference. A prepared specimen is shown in Figure 3.1.

Figure 3.1 Prepared specimen

Fixtures are then placed on each specimen and secured by bolts. It is important that the specimen can spin around each bolt freely but with minimal slack. These fixtures are the contact points with the grips of the fatigue testing machine. After that, an anti-buckling fixture is placed on the remaining portion of the specimen. This step is essential as these specimens can experience out-of-plane buckling under testing loads due to their small thickness. The anti-buckling fixture ensures that the specimen stays flat during the loading

cycles, at least within the crack lengths that meet the LEFM criteria. The anti-buckling fixture is being fastened with the use of a torque screwdriver according to specification. The specimen is then ready for testing. A test-ready specimen is shown in Figures 3.2 and 3.3.

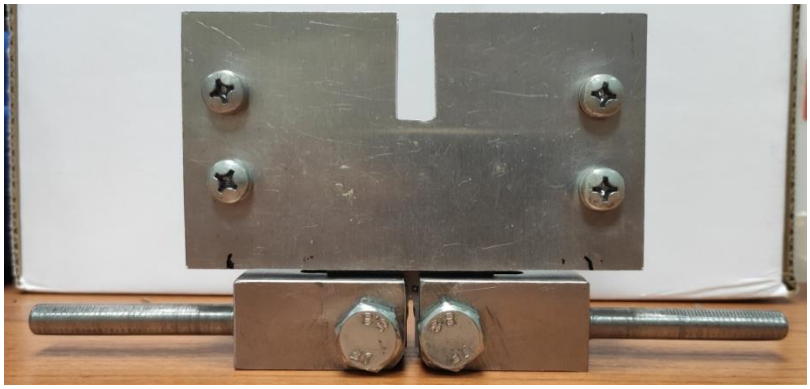

Figure 3.2 Specimen ready for testing

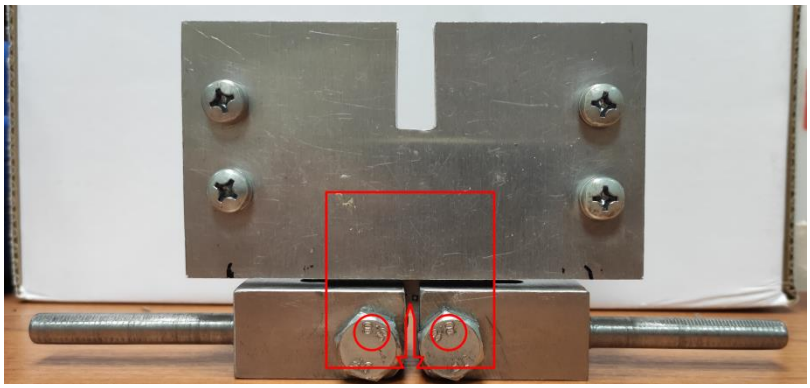

Figure 3.3 Specimen ready for testing (overlay)

3.2 Experimental Setup

The equipment that was used is the following:

- Instron 8801 (100kN) Fatigue Testing System (Figure 3.4)
- Crack Opening Displacement (COD) gauge (Figure 3.5)
- Canon EOS 800D DSLR camera with 65 mm lens (Figure 3.6)
- Laboratory computer

Figure 3.4 Instron Fatigue Testing System

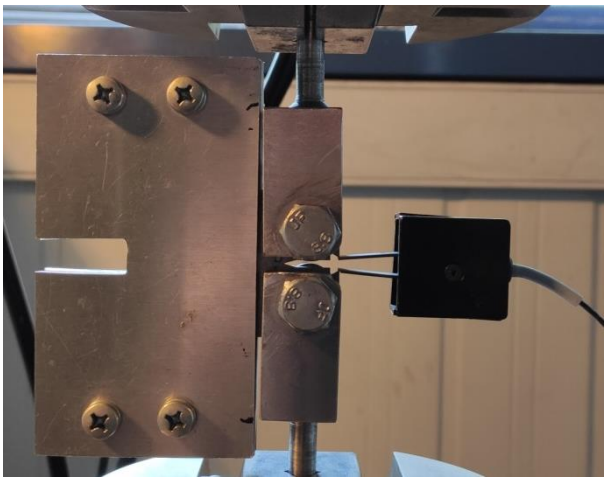

Figure 3.5 COD gauge clipped on a specimen fitted on the fatigue testing machine

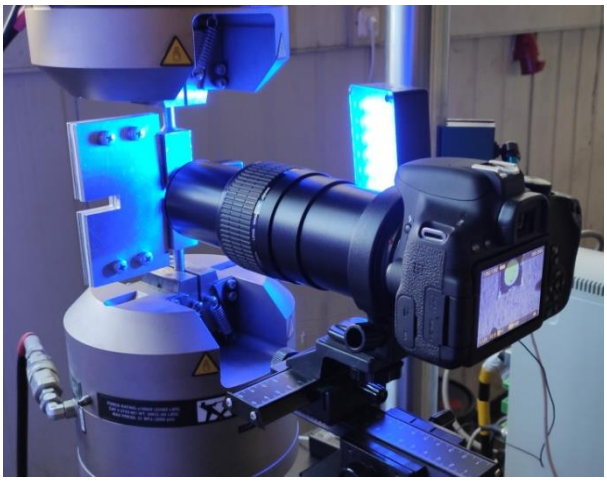

Figure 3.6 DSLR camera and macro lens

After the specimen is prepared, it is fitted on the fatigue testing machine. The camera is then placed and focused on the precrack area of the specimen. The test is now ready to begin.

3.3 Data Processing

After each test, each data set is being checked before the next one to avoid repeating errors. A raw data sample from crack growth tests can be seen in Table 3.1. The data is then processed according to ASTM E 647 Standard [7]. Norman E. Dowling's Mechanical Behavior of Materials [8] gives some valuable insight into data processing as well.

Table 3.1 Raw da/dN data sample from I3 specimen (12-13% pre-strain level, stress ratio $R = 0.1$)

Cycle	Position [mm] MAX	Position [mm] MIN	Load [kN] MAX	Load [kN] MIN	Strain [mm] MAX	Strain [mm] MIN
10	-28.695	-28.736	1.352	0.915	0.0802	0.0575
20	-28.688	-28.736	1.401	0.847	0.0832	0.0547
30	-28.678	-28.735	1.439	0.817	0.0858	0.0531
40	-28.672	-28.73	1.468	0.809	0.0871	0.0528
50	-28.667	-28.73	1.476	0.788	0.0882	0.0523
60	-28.668	-28.728	1.483	0.779	0.0883	0.0519
70	-28.664	-28.728	1.485	0.772	0.0891	0.0517
80	-28.662	-28.725	1.49	0.772	0.0894	0.0513
90	-28.662	-28.726	1.49	0.771	0.0892	0.0515
100	-28.66	-28.724	1.494	0.777	0.0897	0.0519

After processing, we are left with values that correspond to crack lengths a per cycle, which can easily be converted to crack growth rates da/dN, and stress intensity range ΔK. These values can then be plotted accordingly.

3.4 Opening force measurements

As it was previously stated, there are two types of tests that were performed, one to determine crack growth rates (da/dN) and one to measure the crack opening force at various crack lengths. Crack opening force (P_o) measurements take place (where needed) after the pre-crack length has been reached at fixed crack length intervals. In this case every 0.5 mm. Crack propagation is being observed through the camera, as it is shown in Figure 3.7 and 3.8.

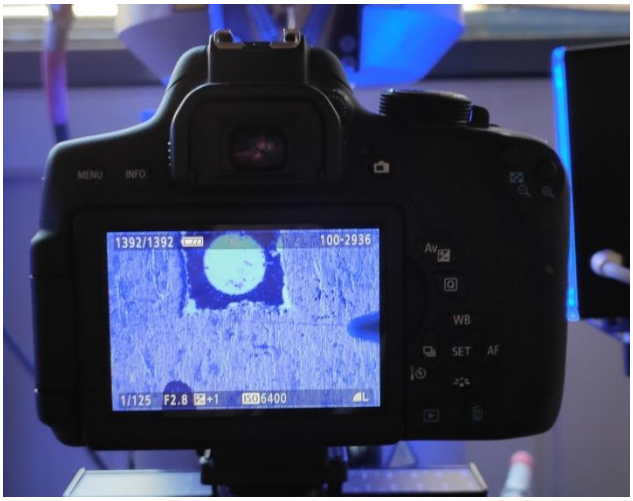

Figure 3.7 Crack examination

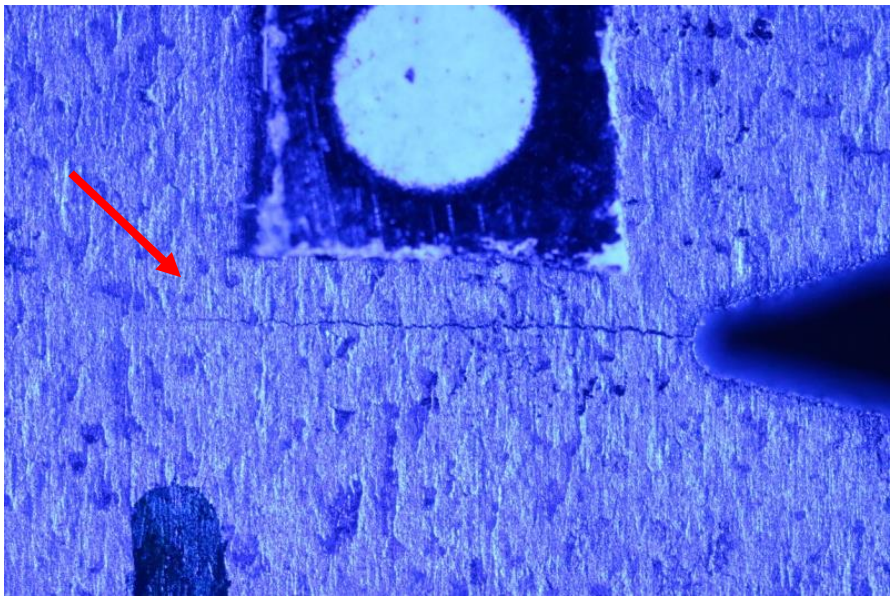

Figure 3.8 Crack initiation snapshot

The da/dN test is paused every time a P_o measurement is being taken. This is done because the test frequency must be dropped extremely low (from 8-10 Hz to 0.3 Hz) to get sufficient data density for the P_o measurements. Extra care has been taken so as to keep test loads within the minimum and maximum values that are set for each test while switching in between the tests.

A raw data sample of opening force measurements can be seen in Table 3.2.

Table 3.2 Raw P_o measurement data sample for J2 specimen (8-9% pre-strain level, stress ratio $R = 0.1$)

Time Sec	Position mm	Load kN	Strain 1 mm	Cycle
0	-26.9041	0.499892	0.0351913	1
0.001	-26.8978	0.50683	0.0355093	1
0.002	-26.9031	0.497746	0.035393	1
0.003	-26.9013	0.499249	0.0353675	1
0.004	-26.9022	0.502253	0.0351717	1
0.005	-26.9033	0.500846	0.0352309	1
0.006	-26.9009	0.49715	0.0353398	1
0.007	-26.9006	0.501311	0.0357299	1
0.008	-26.9006	0.49938	0.0353863	1
0.009	-26.9006	0.500095	0.0353363	1
0.01	-26.9004	0.501823	0.0351679	1

Data from P_o measurements can be used to fill in the missing data from the da/dN test after a small reduction as the sampling rate for each test is quite different. After processing, an opening force value is deduced for each crack length measurement which can then be plotted accordingly.

Chapter 4: Experimental Results

4.1 Fatigue Crack Growth Results

After plotting the data from each test specimen, some comparisons can be made to hopefully observe the effects of pre-existing plastic deformation on crack growth rates. As previously stated, there were performed three test repeats for each test parameters set. Thus, the following points and Paris curves were plotted using data from all three test specimens.

To begin with, Figures 4.1a and 4.2a illustrate the plastic pre-strain effect for each stress ratio R that was used during testing.

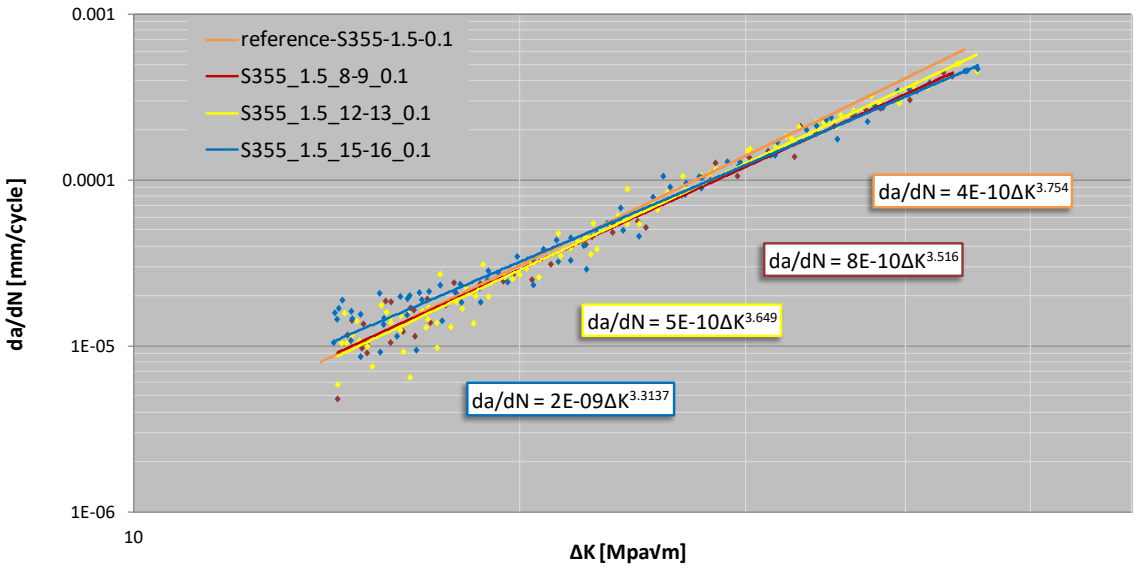

Figure 4.1a da/dN diagram of reference and pre-strained material for stress ratio $R = 0.1$

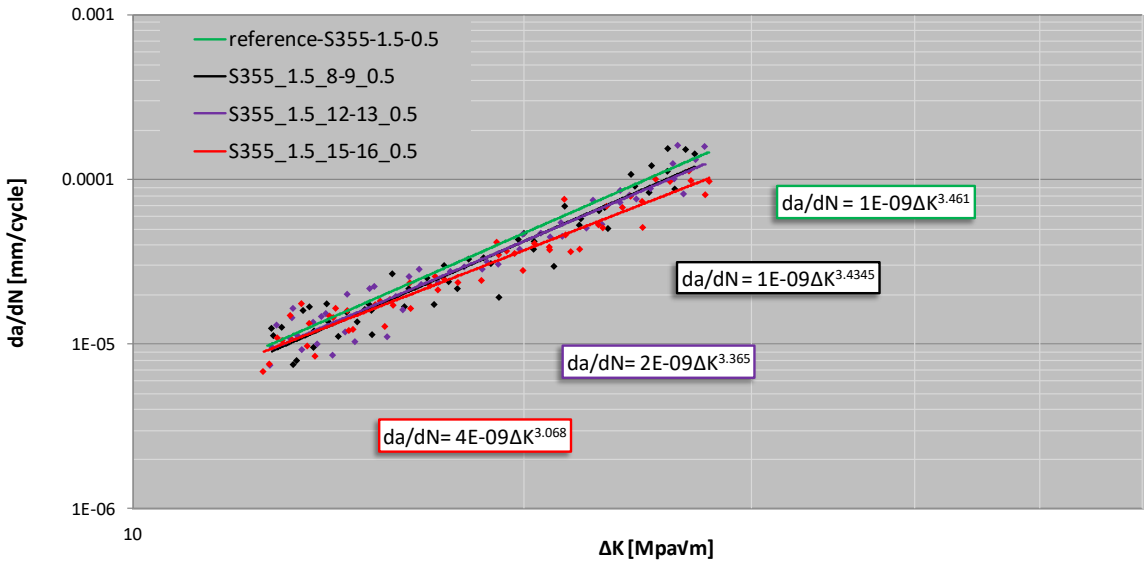

Figure 4.2a da/dN diagram of reference and pre-strained material for stress ratio $R = 0.5$

As we can see, the behavior of the material appears to be similar among the pre-strain levels in general. In order to improve clarity, Figures 4.1b and 4.2b are created using only Paris curves without the data points from which they were generated.

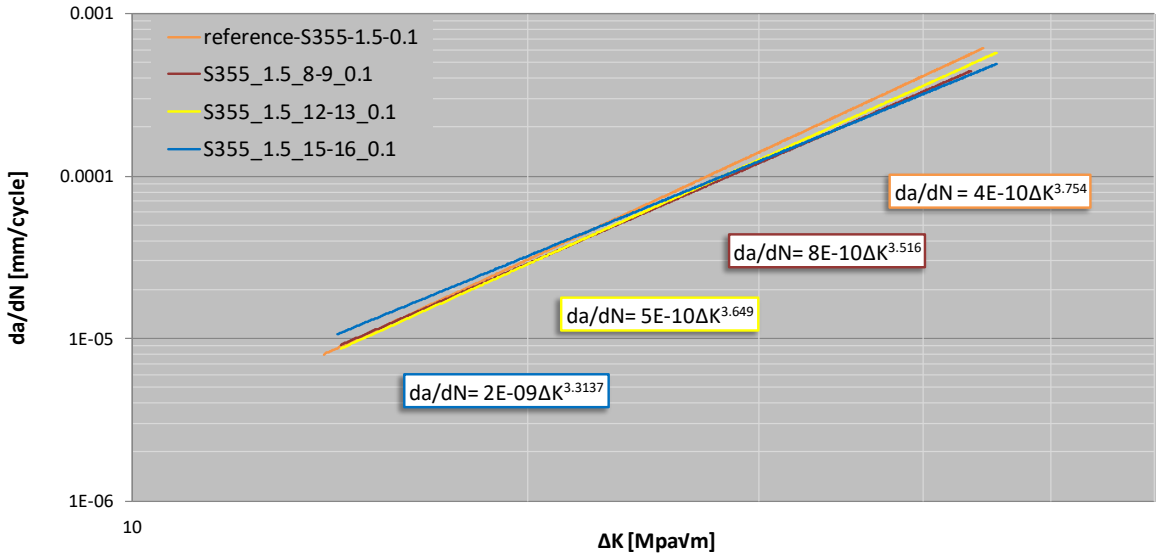

Figure 4.1b Paris curves of reference and pre-strained material for stress ratio $R = 0.1$

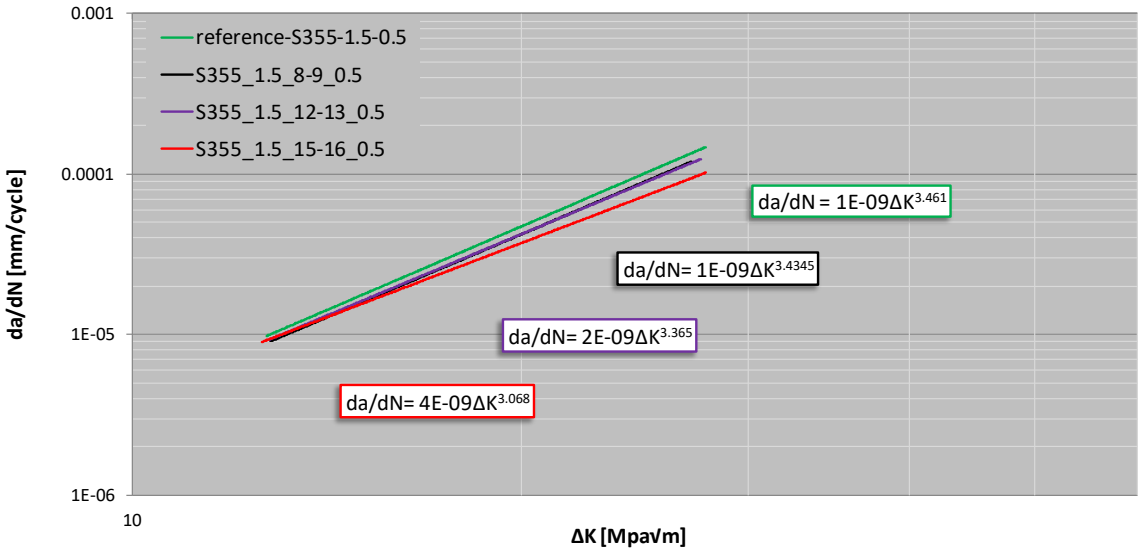

Figure 4.2b Paris curves of reference and pre-strained material for stress ratio $R = 0.5$

For stress ratio $R = 0.1$ there seems to be no significant variation among pre-strain levels. However, it can be observed that for low ΔK values, pre-strain level of 15-16% produces a small increase in crack growth rates. Also, for high ΔK values there is a small decrease in crack growth rates as pre-strain levels increase. Moreover, there seems to be a small decrease in the m exponent of each Paris equation as pre-strain levels increase.

Likewise, for stress ratio $R = 0.5$, low ΔK values produce similar crack growth rates while in high ΔK values, da/dN and the exponent m show a slight decrease as pre-strain levels increase.

Following, Figures 4.3, 4.4, 4.5 and 4.6 depict the stress ratio effect for reference material and each pre-strain level respectively.

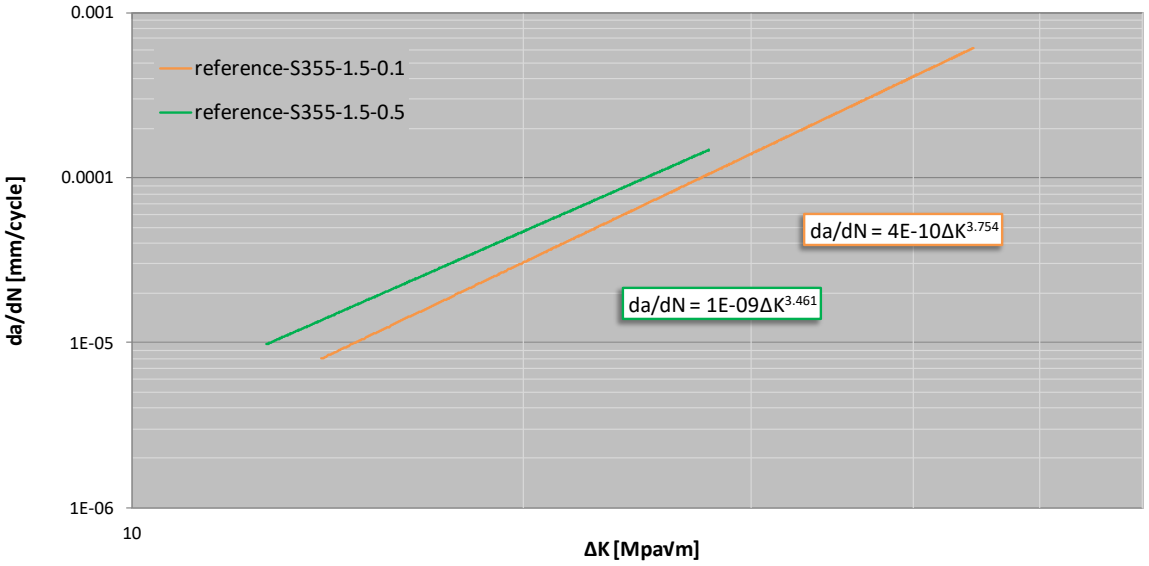

Figure 4.3 Stress ratio R effect on crack growth rates for reference material

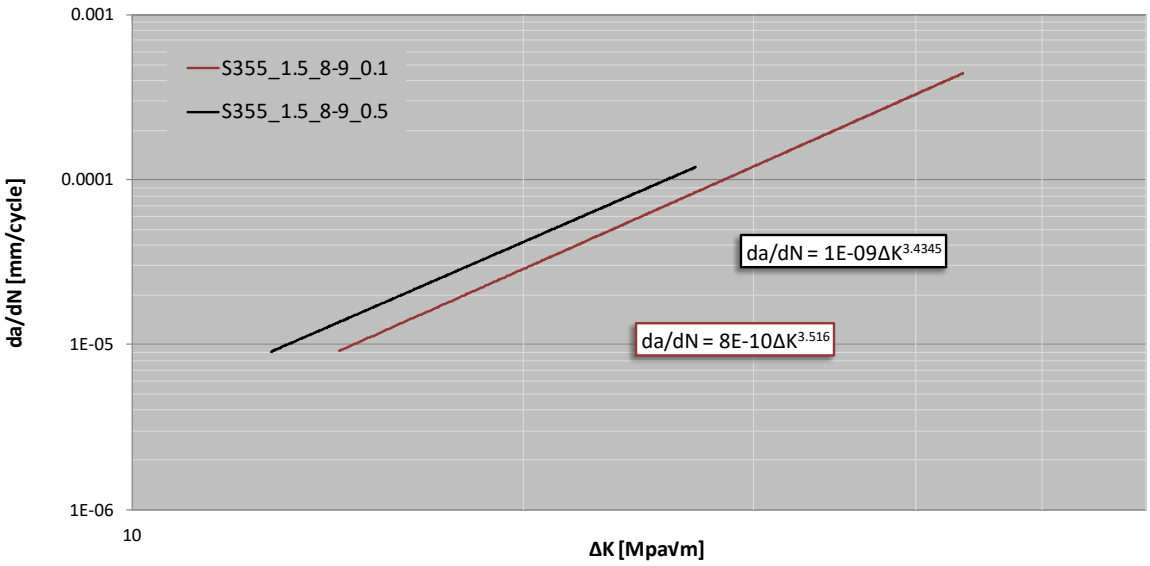

Figure 4.4 Stress ratio R effect on crack growth rates for 8-9% pre-strain level

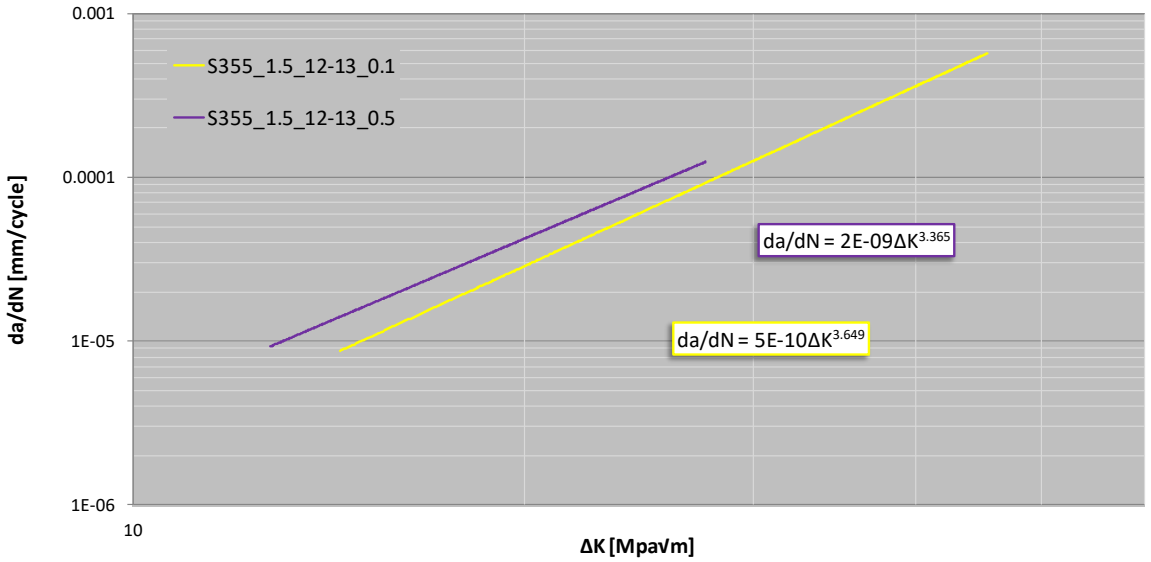

Figure 4.5 Stress ratio R effect on crack growth rates for 12-13% pre-strain level

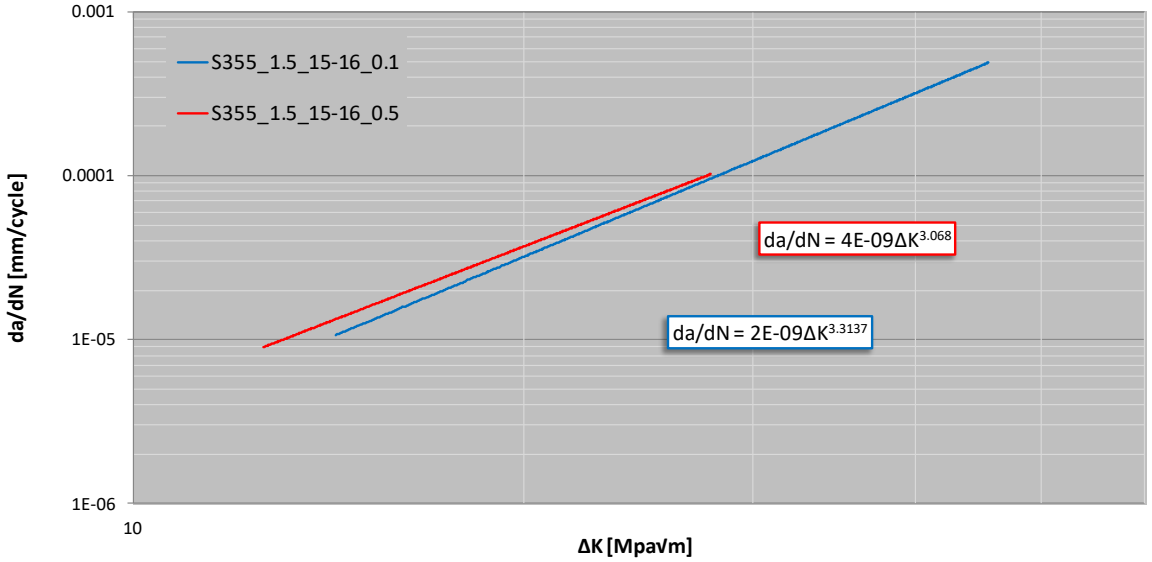

Figure 4.6 Stress ratio R effect on crack growth rates for 15-16% pre-strain level

For both reference and pre-strain levels alike, an increase in stress ratio R causes growth rates for a given ΔK value to be larger as the Paris curve shifts upwards. Also, there are small deviations in the exponent m value between the two stress ratios across all pre-strain levels. Another important observation is that as pre-strain levels increase, the distance between the two Paris curves becomes smaller as they appear to almost converge by the last pre-strain level.

4.2 Opening Force Results

We can now compare how the opening force reacts to different amounts of plastic deformation. Figure 4.7 illustrates Po measurements along a range of crack lengths for each pre-strain level that was used for testing.

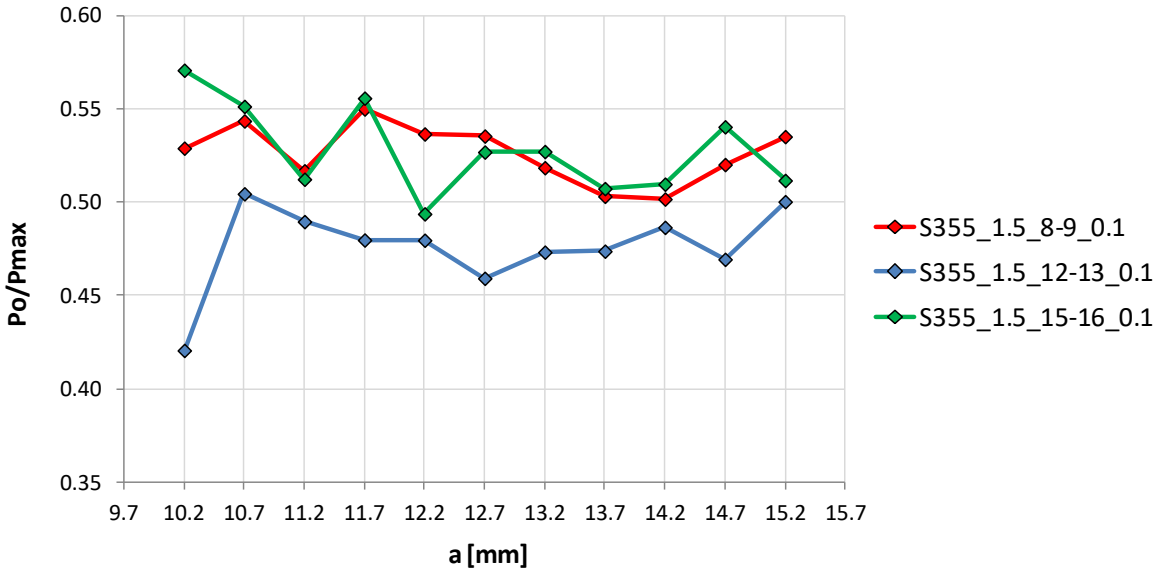

Figure 4.7 Pre-strain effect on crack opening force P_o

As it was previously stated, these measurements were performed only for stress ratio of $R = 0.1$ as the closure effect is more evident under smaller loading forces. P_o/P_{max} values were used for plotting as the maximum loading force is not exactly the same for each test [11]. Opening force P_o values appear to be lower for pre-strain levels of 12-13% in comparison to 8-9% and 15-16% but there is no relative trend among the three pre-strain levels that were examined.

4.3 Discussion

Before coming to any conclusions, it is important to share some details about the testing and the aforementioned results.

First, we shall investigate whether pausing the da/dN test to perform P_o measurements affects crack growth rates. In order to do that, the following a-N graph in Figure 5.1 can prove useful.

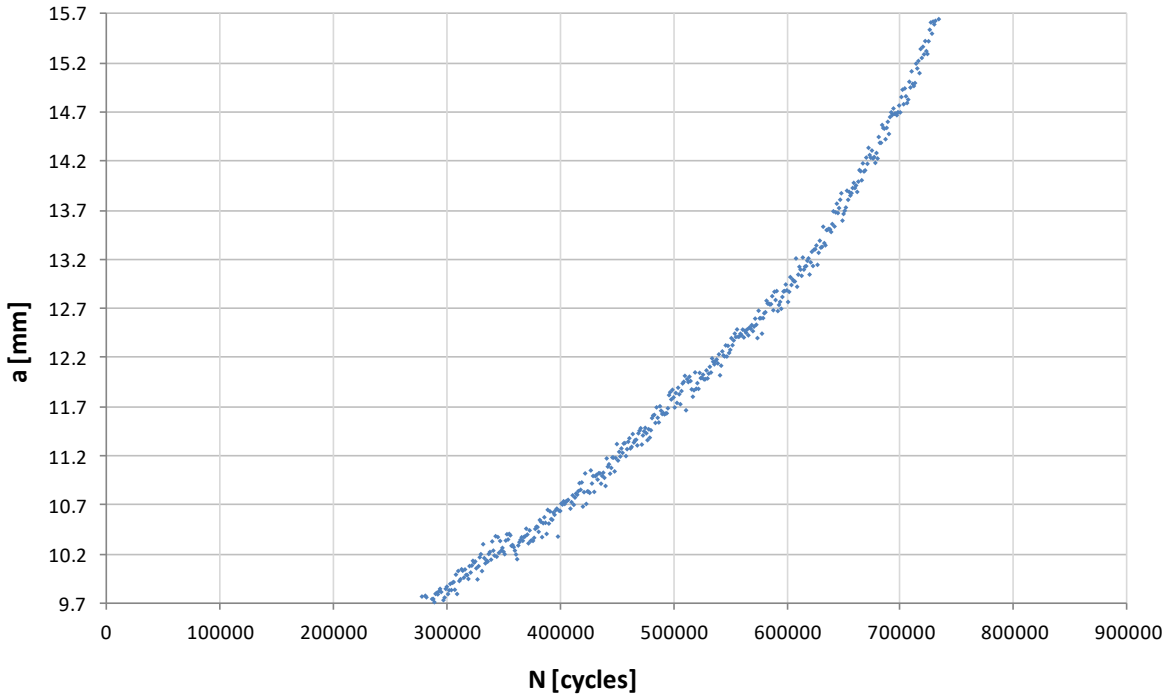

Figure 4.8 a-N curve for 12-13% pre-strain level

Crack length values are produced according to E 647 standard [7] using data from the COD gauge. Also, P_o measurements take place every 0.5 mm from 10.2 mm to 15.2 mm as the crack is monitored visually and the anti-buckling obstructs visual contact with cracks above 15.5 mm. Having said that, as it is illustrated above, crack propagation seems to decelerate slightly after some P_o measurement but quickly picks up pace returning to its initial behavior before pausing the test. Therefore, it is safe to assume that opening force measurements do not have a significant effect over the da/dN test.

In addition, it is important to mention that any result interpretation regarding the P_o measurements remains inconclusive as there was only one test performed for each pre-strain level.

Chapter 5: Conclusions and Future Directions

After examining the observations mentioned in Chapter 4, now is the time to come to some conclusions.

Considering the da/dN tests, the slight decrease in high ΔK crack growth rates and the slope of each Paris curve (exponent m) can be attributed to compressive residual stresses induced to the material by plate stretching [12, pp. 245-247]. As plastic deformation increases, residual stresses increase closing the crack surfaces and retarding crack growth rates. Moreover, as pre-strain levels increase, specimen thickness decreases which increases the critical stress intensity factor K_c [12, pp. 136-137] making the given specimen more fatigue tolerant. However, the material loses ductility and becomes more brittle with the increase of plastic deformation which makes it more vulnerable to fatigue damage [8]. These counteracting effects may explain why there are small observable differences among the pre-strain levels.

As expected, increasing the stress ratio R increases crack growth rates for a given ΔK value [8]. However, the two ($R = 0.1$ and $R = 0.5$) Paris curves converging with the increase of pre-strain levels seems counter-intuitive. As previously stated, the material experiences work hardening by plastic deformation resulting in loss of ductility making it more brittle. However, R effect is more pronounced for more brittle materials [8]. Thus, if that was the case, an increase of R would increase the distance between the two Paris curves as pre-strain levels increase. Maybe as pre-strain levels and residual stresses increase, the opening force P_o increases as well. Given that the maximum loading force P_{max} remains practically the same in each test (for a given R), an increase in P_o would decrease the effective force range ΔP_{eff} given by Eq. 6.1 [7].

$$\Delta P_{eff} = P_{max} - P_o \tag{6.1}$$

Therefore, we can assume that as ΔP_{eff} decreases with increasing pre-strain levels, R effect becomes less pronounced which would explain why the two Paris curves converge.

As far as the P_o measurements go, as it was stated, the material is subjected to strain hardening as the pre-strains increase [13], and as a result, the yield strength is increased as well. However, higher yield strength will induce smaller plastic zones and consequently less crack closure [14]. So in reality, the opening force is expected to decrease as pre-strain levels increase. That can maybe be observed in Figure 4.7 as opening force measurements for 8-9% are greater than those for 12-13% but there is no clear trend among the three pre-strain levels. Perhaps the coexistence of residual stresses and strain hardened material produces mixed results.

Also, it must be reminded that results on this part of the study remain inconclusive due to the absence of test repeats in any pre-strain level. More testing is needed to get the full picture of the crack closure phenomenon.

Having said all that, there are some directions for future work. It would be interesting to investigate other phenomena like crack-initiation using replication methods and how different pre-strain levels affect them. Of course more testing must be performed to make any reliable assumptions about the crack closure effect. It would be also interesting to study different materials and a greater range of pre-strain levels and stress ratios to get a clearer view on their effects.

References

[1] Material Fatigue, COMSOL [https://www.comsol.com/multiphysics/material-fatigue?parent=structural-mechanics-0182-242]

[2] Cold-formed steel, Wikipedia [https://en.wikipedia.org/wiki/Cold-formed_steel]

[3] Fastcold – Research and Design, FASTCOLD [https://fastcold-rfcs.com/]

[4] Nick Gilbert, Structural Steel - S235, S275, S355 Chemical Composition, Mechanical Properties and Common Applications, 2012 [https://www.azom.com/article.aspx?ArticleID=6022]

[5] European Steel and Alloy Grades/Numbers, SteelNumber [http://www.steelnumber.com/en/steel_composition_eu.php?name_id=206]

[6] SSAB Domex, SSAB Domex 355MC [https://www.ssab.com/products/brands/ssab-domex/products/ssab-domex-355mc]

[7] ASTM E647-00, Standard Test Method for Measurement of Fatigue Crack Growth Rates, ASTM International, West Conshohocken, PA, 2000, [https://www.astm.org/]

[8] Norman E. Dowling, Fatigue Crack Growth, *Mechanical Behavior of Materials,* 4th Edition, Pearson, Essex, pp. 560-624, 2013

[9] Hadžalić Mustafa, Oruc Mirsada, Sunulahpašić Raza, (2014), Analysis of Stress-Strain State and Life Prediction of Notched Structural Components of Mine Hoists, September, 2014

[10] Christos G. Prosgolitis, Alexis T. Kermanidis, Spyros A. Karamanos, Comparative study of fatigue crack propagation in S355 and S460 structural steels. (Oral presentation at 7th Panhellenic Congress, Athens, Greece, 11-13 December 2019)

[11] Andreas Tzamtzis, *Fatigue crack growth prediction under mode I loading in friction stir aluminum alloy weld*, Doctor of Philosophy in Mechanical Engineering Dissertation, University of Thessaly, 2015

[12] Ralph I. Stephens, Ali Fatemi, Robert R. Stephens, Henry O. Fuchs, *Metal Fatigue in Engineering*, 2nd Edition, John Wiley & Sons, Canada, 2000

[13] Ma JL, Chan TM, Young B. (2015) Material properties and residual stresses of cold-formed high strength steel hollow sections. *Journal of Constructional Steel Research*, 109, p. 157

[14] Schijve J. (1976) The effect of pre-strain on fatigue crack growth and crack closure, *Engineering Fracture Mechanics*, 8, p. 580